HHS Public Access

Author manuscript

J Surg Oncol. Author manuscript; available in PMC 2022 December 01.

Published in final edited form as:

J Surg Oncol. 2021 December ; 124(7): 1121–1127. doi:10.1002/jso.26623.

Rapid tumor-labeling kinetics with a site-specific near-infrared anti-CEA nanobody in a patient-derived orthotopic xenograft mouse model of colon cancer

Thinzar M. Lwin, MD[1,2], **Michael A. Turner, MD**[1,3], **Siamak Amirfakhri, PhD**[1,3], **Hiroto Nishino, MD, PhD**[1,3], **Pieterjan Debie**[4], **Bard C. Cosman, MD**[1,3], **Robert M. Hoffman, PhD**[1,3,5], **Sophie Hernot, PhD**[4], **Michael Bouvet, MD**[1,3]

[1]Department of Surgery, University of California San Diego, San Diego, California, USA

[2]Department of Surgical Oncology, Dana Farber Cancer Center, Boston, Massachusetts, USA

[3]VA San Diego Healthcare System, San Diego, California, USA

[4]Laboratory for In vivo Cellular and Molecular Imaging (ICMI-BEFY-MIMA), Vrije Universiteit Brussel, Brussels, Belgium

[5]AntiCancer, Inc., San Diego, California, USA

Abstract

Background/Objectives: Nanobodies are the smallest biologic antigen-binding fragments derived from camelid-derived antibodies. Nanobodies effect a peak tumor signal within minutes of injection and present a novel opportunity for fluorescence-guided surgery (FGS). The present study demonstrates the efficacy of an anti-CEA nanobody conjugated to near-infrared fluorophore LICOR-IRDye800CW for rapid intraoperative tumor labeling of colon cancer.

Methods: LS174T human colon cancer cells or fragments of patient-derived colon cancer were implanted subcutaneously or orthotopically in nude mice. Anti-CEA nanobodies were conjugated with IRDye800CW and 1–3 nmol were injected intravenously. Mice were serially imaged over time. Peak fluorescence signal and tumor-to-background ratio (TBR) were recorded.

Results: Colon cancer tumors were detectable using fluorescent anti-CEA nanobody within 5 min of injection at all three doses. Maximal fluorescence intensity was observed within 15 min–3 h for all three doses with TBR values ranging from 1.3 to 2.3. In the patient-derived model of colon cancer, fluorescence was detectable with a TBR of 4.6 at 3 h.

Conclusions: Fluorescent anti-CEA nanobodies rapidly and specifically labeled colon cancer in cell-line-based and patient-derived orthotopic xenograft (PDOX) models. The kinetics of nanobodies allow for same day administration and imaging. Anti-CEA-nb-800 is a promising and practical molecule for FGS of colon cancer.

Correspondence: Michael Bouvet, MD, University of California San Diego, Moores Cancer Center, 3855 Health Sciences Dr #0987, La Jolla, CA 92093-0987, USA. mbouvet@ucsd.edu.

Keywords

anti-CEA nanobody; fluorescence-guided surgery; fluorescent anti-CEA nanobody; patient-derived orthotopic xenograft models; tumor-specific fluorescence

1 | INTRODUCTION

Colorectal cancer (CRC) remains one of the most common cancer diagnoses in the United States with 147,950 new cases diagnosed each year.[1] Surgical resection is the primary curative treatment modality. Resection with an R0 margin, meaning no gross or microscopic tumor cells are left in the surgical bed, is the primary aim.

There is currently intense interest in fluorescence-guided surgery (FGS) of cancer. Using tumor-specific molecules conjugated to near-infrared fluorophores, a fluorescence signal can be directed at the tumor.[2] Tumor-targeting molecules can be antibodies, antibody fragments, or peptides.[3] The tumor-specific fluorescence signal can be used for intra-operative visualization of the tumor, margins, surgical bed and any satellite lesions or metastasis.

The human carcino-embryonic antigen (CEA) or CECAM5 is a well-characterized tumor antigen that is absent in normal adult tissue, and is highly expressed in a number of solid GI malignancies.[4] Our lab has pioneered the use of FGS with patient-like mouse models of cancer using anti-CEA antibodies. We showed that the technology is a great benefit to effective R0 resections and can reduce or eliminate recurrence and increase survival in preclinical models.[5–9] SGM-101, an anti-CEA antibody conjugated to a near-infrared fluorophore, has been evaluated in Phase I and II clinical trials.[10,11] It has been shown to be safe and efficacious in visualizing tumors for surgical navigation. SGM-101 is currently undergoing a Phase III multi-centered clinical trial for use in surgical navigation during surgery for colorectal malignancies including peritoneal surface malignancies (NCT03659448).

Although antibodies are well developed reagents for tumor targeting, they have a large molecular size which leads to impedance in tumor penetration and a delay in timing of visualization of up to 24–48 h. In clinical use, this leads to the need for a separate clinical visit for the purpose of probe administration which can be a barrier in adoption of this technology.

Nanobodies are the smallest biologic antigen-binding fragments. They are derived from camelid-derived antibodies made of only heavy chains.[12] Nanobodies have been shown to penetrate tumors with greater efficiency compared to intact antibodies and can produce a peak signal within hours of injection when conjugated to a fluorophore or radionuclide.[3,13] This makes nanobodies ideal probes for same-day administration and visualization.

In the present study, we demonstrate an anti-CEA nanobody conjugated to an 800 nm fluorophore (LICOR-IRDye800CW) to target human colorectal tumors in mouse models and label them rapidly and brightly.

2 | MATERIALS AND METHODS

2.1 | Cell culture

The human colon cancer cell line LS-174T (ATCC® CL-188™), was maintained in Roswell Park Memorial Institute 1640 (RPMI-1640) medium (Gibco-BRL). The medium was supplemented with 10% fetal calf serum (Hyclone), 1% L-Glutamine, and 1% penicillin/streptomycin (Gibco-BRL). The cells were incubated at 37°C in a 5% CO_2 incubator.

2.2 | Nanobody synthesis and conjugation

An anti-CEA (NbCEA5) was synthesized as described previously.[14–16] Briefly, the nanobody constructs with a carboxy-terminal cysteine tag were cloned into a pHEN6c plasmid and expressed in *Escherichia coli*. Nanobody products were purified from periplasmic extracts using an immobilized metal affinity chromatography followed by subsequent size-exclusion chromatography. The purified nanobodies were reduced and subsequently incubated at pH 7 with a 5-fold molar excess of IRDye 800CW-Maleimide (LICOR Biosciences).[17] The fluorescently-labeled nanobodies were purified using size exclusion chromatography. The purified fluorophore-conjugated nanobody is called aCEA-nb-800.

2.3 | Animal care

Immunocompromised nude nu/nu mice were obtained from Jackson Labs and maintained in a barrier facility on high-efficiency particulate air (HEPA)-filtered racks. Mice were maintained on an autoclaved laboratory rodent diet (Teckland LM-485; Western Research Products) and kept on a 12 h light/12 h dark cycle. All surgical procedures and intravital imaging were performed with the animals anesthetized by intramuscular injection of an anesthetic cocktail composed of ketamine 100 mg/kg (MWI Animal Health), xylazine 10 mg/kg (VWR), and acepromazine 3 mg/kg (Sigma). Animal procedures were performed under VA-approved animal protocol A17-020. All animal studies were conducted in accordance with the principles and procedures outlined in the NIH Guide for the Care and Use of Animals.

2.4 | Establishment of a patient-derived orthotopic xenograft mouse model

Samples from colon cancers of patients undergoing surgical resection at the VA San Diego Healthcare System under an Institutional Review Board (IRB) approved protocol #18-42. Patients signed informed consent for tissue collection and research at their clinic visit before their surgery. Tumor fragments were collected and implanted subcutaneously over the flanks of nude mice. Subcutaneous tumors were monitored twice a week and allowed to grow for 4–8 weeks to develop patient-derived xenograft mouse models (PDX). Once the subcutaneous tumors were large enough to supply adequate tumor for orthotopic implantation, approximately 7–10 mm, the subcutaneous tumors were harvested and surgically engrafted onto the cecum of recipient nude mice using a surgical orthotopic implantation (SOI) technique developed for colon cancer.[18]

2.5 | In vivo imaging studies

LS-174T human colon cancer cells (1×10^6 cells per animal) were injected subcutaneously into four separate subcutaneous locations in the shoulder and flanks of nude mice. The tumors were allowed to grow for 4 weeks or until 5–7 mm in size. For the dose and time response evaluation of the anti-CEA nanobody, doses of 1, 2, 3 nmol of anti-CEA-nb-800 were injected intravenously into mice bearing subcutaneous tumors. Mice were sequentially imaged at 5 min, 10 min, 15 min, 30 min, 1 h, 2 h, 3 h, 24 h, and daily for 4 days after injection. This was repeated with the subcutaneous implant of the patient-derived colon cancer tumor.

For in-situ evaluation of orthotopic colon cancer xenografts, mice were injected intravenously with 3 nmol of aCEA-nb-800. Mice were sacrificed at 3 h and a midline laparotomy and the orthotopic tumor exteriorized for imaging.

Images were acquired at the IRDye800 wavelength using the Pearl Trilogy Small Animal Imaging System (LI-COR Biosciences). Peak fluorescence intensity was obtained at a region of interest using Image Studio software (LI-COR Biosciences).

2.6 | Statistics

Tumor-to-background ratio (TBR) was calculated by dividing the maximal fluorescence intensity (MFI) at the tumor by the MFI at adjacent skin (sub-cutaneous imaging) or viscera (intra-vital imaging). Data are reported as mean ± standard error of the mean (*SEM*). Standard error bars are indicated in figures.

3 | RESULTS

Noninvasive imaging of subcutaneous LS174T colon cancer xenografts showed that the tumors were detectable using the aCEA-cnb-800 within 5 min of injection of the probe at all three doses evaluated. The results are summarized in Figure 1. The lowest 1 nmol dose of nanobody, resulted in MFI of 0.95 (*SEM* ± 0.17) at 30 min and a TBR of 1.8 at that time point (*SEM* ± 0.45). At this 1 nmol dose, the highest TBR was 7 (*SEM* ± 3.7) at 72 h. The intermediate 2 nmol dose of nanobody resulted in a peak fluorescence intensity of 1.9 (*SEM* ± 0.08) at 3 h with a TBR of 2 at that time point (*SEM* ± 0.37). At this 2 nmol dose, the highest TBR was at 2.8 (*SEM* ± 0.25) at 48 h. The highest 3 nmol dose of nanobody resulted in an MFI of 1.9 (*SEM* 0.36) at 3 h with a TBR of 2.3 at that time point (*SEM* ± 0.33). At the 3 nmol dose, the highest TBR was at 5.6 at 24 h (*SEM* ± 1.13).

Intra-vital imaging of LS174T orthotopic tumors was performed 3 h after administration of 3 nmol of aCEA-nb-800. Bright light gray scale imaging showed the primary tumor with a red arrow (Figure 2A). Multiple sub-millimeter satellite lesions were detectable. These lesions were very difficult to visualize on the bright light image (Figure 2A blue arrows). Fluorescence imaging showed clear labeling of the primary tumor as well as satellite tumors on the color-overlay mode (Figure 2B) and the fluorescence signal only mode (Figure 2C). The mean TBR for the primary tumor using the adjacent cecum as the background was 5.5 (*SEM* ± 1.30).

The peak fluorescence signal over time of the skin, kidney, liver and the tumor for subcutaneous implantation of the patient-derived xenograft are summarized in Figure 3. Based on the LS174T time course imaging, a dose of 3 nmol of aCEA-nb-800 was used, the peak fluorescence intensity was 1.3 (*SEM* ± 0.27) at 3 h. At this time point, the TBR was 2.7 (*SEM* ± 0.28). The max TBR was at 3.5 (*SEM* ± 0.89) at 48 h.

Intra-vital imaging of colon cancer patient-derived orthotopic xenograft mouse models was performed 3 h after administration of 3 nmol of aCEA-nb-800. Bright-light imaging shows the primary tumor with a red arrow (Figure 4A). The tumor border is difficult to delineate from the surrounding tissue. Fluorescence imaging (Figure 4B,C, RED arrow) shows clear labeling of the primary tumor. No satellite tumors were seen in this model. There is a strong fluorescence signal from the kidney indicating renal elimination of the probe (Figure 4, blue asterisk). The MFI was 1.2 (*SEM* ± 0.15) with a mean TBR of 4.6 (*SEM* ± 1.47) using the adjacent cecum as the background.

4 | DISCUSSION

Accurate visualization of colon cancer and complete resection during surgery is critical. Positive tumor margins lead to early recurrence and overall poor overall outcomes and survival, with a hazard ratio of 3.39 for survival.[19] Circumferential resection margin involvement leads to a 50%–99% risk of recurrence[20,21] and as well as increased cancer-specific mortality, irrespective of lymph node involvement.[22,23] This is especially important as a majority of colorectal surgeries are performed minimally invasively and tactile feedback for palpation of the tumor is limited or non-existent. Image contrast with fluorescence could enhance surgical visualization of the tumor and can potentially increase the rate of R0 resection. Many modalities exist to deliver tumor-specific fluorescence and the number of clinical trials using tumor-specific fluorescent probes are rapidly increasing.[3] Fluorescent nanobodies are a promising new modality for labeling colon cancer.

The aCEA-nb-800 rapidly and successfully labeled CEA expressing colon cancer in both cell line-based tumors and PDOX tumors. The probe was specific for the tumor and showed a rapid accumulation by the tumor within minutes of intravenous injection.

Time course imaging using different doses over time with the LS174T subcutaneous tumors showed that MFI was achieved within 30 min for the 1 nmol dose and within 3 h for both 2 and 3 nmol doses (Figure 1A). Although maximal fluorescence intensity with 2 nmol of aCEA-nb-800 was slightly higher than with 3 nmol at some time points, the error bars overlap, and we do not believe that there is a significant difference between these two doses. Highest contrast and highest TBR was observed anywhere from 24 to 72 h later (Figure 1B,C). MFI within minutes to hours is consistent with the existing literature on nanobodies which show peak signals within hours and a sharp decline thereafter.[17,24–26] The present study is unique in that further time points into days were observed and recorded and we observed some tumor-specific signal persisting well into 120 h. However, a high contrast must be balanced with a bright signal intensity. This is similarly reflected in the time course imaging using a PDOX model of colon cancer which showed the brightest signal with MFI of 1.3 at 3 h with a reasonable TBR of 2.7 (Figure 3). The maximal TBR of 3.5 was

achieved at a later time point of 48 h. Therefore, with the goal of achieving a bright signal with a reasonable contrast, a time point of 3 h and a dose of 3 nmol was selected for the PDOX experiments. While further time points between 3 and 24 h were not recorded for these experiments, these would be interesting to evaluate in the future. This would help further delineate the potential of repeat dosing in a molecule that is eliminated rapidly.

LS174T colon cancer tumor fragments were orthotopically implanted into the cecum of mice to create a more surgical setting of the tumor. The probe had to be delivered from the intravascular circulation, through the neovasculature recruited by the surgically implanted tumor, and retained by the tumor at the time of imaging. The probe labeled not only the primary tumor but satellite tumors (Figure 2). These tiny satellite tumors are barely visible on the bright-light image, but clearly well contrasted in the fluorescence image (Figure 2A vs. 2B,C). The technology is not only useful for visualization of the primary lesion but can be useful to visualize peritoneal carcinomatosis.

Orthotopic implantation of patient-derived xenografts more closely represents the original tumor in the patient and mimic the heterogeneity of tumor tissue compared to cell line-based tumors.[27] In the PDOX model of colon cancer, the MFI was 1.2 and the mean TBR was 4.6 at 3 h. There was a strong fluorescence signal from the tumor. The margin and tissue interface between the normal colon and the tumor are clearly visible using fluorescence enhancement. There was a very strong fluorescence signal from the kidney. This is due to the renal elimination mechanism of the probe. While it can also be useful for colorectal surgery in helping clearly identify the ureters and bladder, it can be confounding for visualization of tumors and the tumor bed anterior to the kidneys and the molecule. The use of nanobodies for tumor-specific FGS in this anatomic area must be considered carefully. However, in mice, there is minimal peri-nephric fat over the kidneys. In humans, this may be less of an issue as the peri-nephric fat pad is more substantial. With this known renal elimination mechanism, kidneys can be shielded or gently retracted away from the region of interest.

Nanobodies show important clinical promise for delivery of tumor-specific fluorescence. The rapid pharmacokinetic of nanobodies are ideal for same-day administration. Nanobodies retain their avidity and ease of bioengineering similar to antibodies. They are able to bind deeper clefts and motifs due to their small size.[28] As well as ease of engineering due to their short sequence, nanobodies have high thermal and chemical stability for alternative conjugation strategies to fluorophores.[29] Nanobodies can be cost effective as they are produced in *E. coli* and can be purified with minimal lipo-polysaccharide (LPS) contamination.[30] Caplacizumab is an anti-von Willebrand factor (vWF) therapeutic nanobody, developed for the treatment of thrombotic thrombocytopenic purpura (TTP). It is the most developed nanobody, having completed Phase III clinical trials.[31,32] Nanobodies have also been studied for tumor-specific radio-nuclide imaging in the clinic. Anti-human epidermal growth factor 2 (HER2) nanobodies conjugated to radiotracers (I-131 and Ga-68) were used to image patients with metastatic breast cancer and found to be efficacious. This molecule has completed Phase I clinical trials and is undergoing Phase II clinical trials.[33,34]

The aCEA-nb-800 probe is clinically promising as it is feasible for use in conjunction with FDA-cleared 800 nm near-infrared fluorescence imaging devices such as da Vinci firefly and the Stryker AIM as demonstrated in our previous work in mouse models of pancreatic cancer.[24]

5 | CONCLUSION

Fluorescent anti-CEA nanobodies rapidly and specifically labeled colon cancer in both cell-line-based and patient-derived subcutaneous and PDOX mouse models. Nanobodies are novel and interesting new platforms with important advantages over antibodies for tumor-specific fluorescence labeling. Nanobodies enable tumor-labeling kinetics with the rapidity of nonspecific dyes such as indocyanine green, but with tumor-binding specificity of antibodies. Nanobody technology can be translated to the clinic for same-day labeling and imaging of tumors which avoids a separate visit for the administration of the probe due to very rapid labeling which is not possible with antibodies. The results of the study can be rapidly translated to the clinic for fluorescence-guided surgery to improve the outcome of surgery for colorectal cancer, including liver metastases. The anti-CEA-nb-800 is a promising molecule for fluorescence-guided surgery.

ACKNOWLEDGMENTS

The study was supported by VA Merit Review grant numbers 1 I01 BX003856-01A1 and 1 I01 BX004494-01 (Michael Bouvet), NIH/NCI T32CA121938 (Thinzar M. Lwin and Michael A. Turner), P30 2P30CA023100-28 (UCSD Cancer Center Microscopy).

Funding information

VA merit review, Grant/Award Number: 1 I01 BX003856-01A1; National Cancer Institute, Grant/Award Numbers: 2P30CA023100-28, CA109949, CA132971, T32CA121938

REFERENCES

1. Siegel RL, Miller KD, Jemal A. Cancer statistics, 2020. CA Cancer J Clin 2020;70:7–30. 10.3322/caac.21590 [PubMed: 31912902]
2. Rosenthal EL, Warram JM, de Boer E, et al. Successful translation of fluorescence navigation during oncologic surgery: a consensus report. J Nucl Med Off Publ Soc Nucl Med 2016;57:144–150. 10.2967/jnumed.115.158915
3. Hernot S, van Manen L, Debie P, Mieog JSD, Vahrmeijer AL. Latest developments in molecular tracers for fluorescence image-guided cancer surgery. Lancet Oncol 2019;20:e354–e367. 10.1016/S1470-2045(19)30317-1 [PubMed: 31267970]
4. Hammarström S The carcinoembryonic antigen (CEA) family: structures, suggested functions and expression in normal and malignant tissues. Semin Cancer Biol 1999;9:67–81. 10.1006/scbi.1998.0119 [PubMed: 10202129]
5. Metildi CA, Kaushal S, Pu M, et al. Fluorescence-guided surgery with a fluorophore-conjugated antibody to carcinoembryonic antigen (CEA), that highlights the tumor, improves surgical resection and increases survival in orthotopic mouse models of human pancreatic cancer. Ann Surg Oncol 2014;21:1405–1411. 10.1245/s10434-014-3495-y [PubMed: 24499827]
6. Metildi CA, Kaushal S, Luiken GA, Talamini MA, Hoffman RM, Bouvet M. Fluorescently labeled chimeric anti-CEA antibody improves detection and resection of human colon cancer in a patient-derived orthotopic xenograft (PDOX) nude mouse model. J Surg Oncol 2014;109:451–458. 10.1002/jso.23507 [PubMed: 24249594]

7. Metildi CA, Kaushal S, Luiken GA, Hoffman RM, Bouvet M. Advantages of fluorescence-guided laparoscopic surgery of pancreatic cancer labeled with fluorescent anti-CEA antibodies in an orthotopic mouse model. J Am Coll Surg 2014;219:132–141. 10.1016/j.jamcollsurg.2014.02.021 [PubMed: 24768506]
8. Metildi CA, Kaushal S, Snyder CS, Hoffman RM, Bouvet M. Fluorescence-guided surgery of human colon cancer increases complete resection resulting in cures in an orthotopic nude mouse model. J Surg Res 2013;179:87–93. 10.1016/j.jss.2012.08.052 [PubMed: 23079571]
9. DeLong JC, Murakami T, Yazaki PJ, Hoffman RM, Bouvet M. Near-infrared-conjugated humanized anti-carcinoembryonic antigen antibody targets colon cancer in an orthotopic nude-mouse model. J Surg Res 2017;218:139–143. 10.1016/j.jss.2017.05.069 [PubMed: 28985840]
10. Boogerd LSF, Hoogstins CES, Schaap DP, et al. Safety and effectiveness of SGM-101, a fluorescent antibody targeting carcinoembryonic antigen, for intraoperative detection of colorectal cancer: a dose-escalation pilot study. Lancet Gastroenterol Hepatol 2018;3: 181–191. 10.1016/S2468-1253(17)30395-3 [PubMed: 29361435]
11. Framery B, Gutowski M, Dumas K, et al. Toxicity and pharmacokinetic profile of SGM-101, a fluorescent anti-CEA chimeric antibody for fluorescence imaging of tumors in patients. Toxicol Rep 2019;6: 409–415. 10.1016/j.toxrep.2019.04.011 [PubMed: 31080749]
12. Bathula NV, Bommadevara H, Hayes JM. Nanobodies: the future of antibody-based immune therapeutics. Cancer Biother Radiopharm 2020;36:109–122. 10.1089/cbr.2020.3941 [PubMed: 32936001]
13. D'Huyvetter M, Xavier C, Caveliers V, Lahoutte T, Muyldermans S, Devoogdt N. Radiolabeled nanobodies as theranostic tools in targeted radionuclide therapy of cancer. Expert Opin Drug Deliv 2014; 11:1939–1954. 10.1517/17425247.2014.941803 [PubMed: 25035968]
14. Vaneycken I, Govaert J, Vincke C, et al. In vitro analysis and in vivo tumor targeting of a humanized, grafted nanobody in mice using pinhole SPECT/micro-CT. J Nucl Med 2010;51:1099–1106. 10.2967/jnumed.109.069823 [PubMed: 20554727]
15. Massa S, Xavier C, De Vos J, et al. Site-specific labeling of cysteine-tagged camelid single-domain antibody-fragments for use in molecular imaging. Bioconjug Chem 2014;25:979–988. 10.1021/bc500111t [PubMed: 24815083]
16. Lemaire M, D'huyvetter M, Lahoutte T, et al. Imaging and radio-immunotherapy of multiple myeloma with anti-idiotypic Nanobodies. Leukemia 2014;28:444–447. 10.1038/leu.2013.292 [PubMed: 24166214]
17. Debie P, Van Quathem J, Hansen I, et al. Effect of dye and conjugation chemistry on the biodistribution profile of near-infrared-labeled nanobodies as tracers for image-guided surgery. Mol Pharm 2017;14:1145–1153. 10.1021/acs.molpharmaceut.6b01053 [PubMed: 28245129]
18. Fu XY, Besterman JM, Monosov A, Hoffman RM. Models of human metastatic colon cancer in nude mice orthotopically constructed by using histologically intact patient specimens. Proceedings of the National Academy of Sciences 1991;88(20):9345–9349. 10.1073/pnas.88.20.9345
19. Amri R, Bordeianou LG, Sylla P, Berger DL. Association of radial margin positivity with colon cancer. JAMA Surg 2015;150:890–898. 10.1001/jamasurg.2015.1525 [PubMed: 26132363]
20. Zafar SN, Hu C-Y, Snyder RA, et al. Predicting risk of recurrence after colorectal cancer surgery in the united states: an analysis of a special commission on cancer national study. Ann Surg Oncol 2020; 27:2740–2749. 10.1245/s10434-020-08238-7 [PubMed: 32080809]
21. Liu Q, Luo D, Cai S, Li Q, Li X. Circumferential resection margin as a prognostic factor after rectal cancer surgery: A large population-based retrospective study. Cancer Med 2018;7:3673–3681. 10.1002/cam4.1662 [PubMed: 29992773]
22. Cawthorn SJ, Parums DV, Gibbs NM, et al. Extent of mesorectal spread and involvement of lateral resection margin as prognostic factors after surgery for rectal cancer. Lancet Lond Engl 1990;335: 1055–1059. 10.1016/0140-6736(90)92631-q
23. Wibe A, Rendedal PR, Svensson E, et al. Prognostic significance of the circumferential resection margin following total mesorectal excision for rectal cancer. Br J Surg 2002;89:327–334. 10.1046/j.0007-1323.2001.02024.x [PubMed: 11872058]

24. Lwin TM, Hernot S, Hollandsworth H, et al. Tumor-specific near-infrared nanobody probe rapidly labels tumors in an orthotopic mouse model of pancreatic cancer. Surgery 2020;168:85–91. 10.1016/j.surg.2020.02.020 [PubMed: 32370916]
25. Kijanka MM, Van Brussel AS, Van der Wall E, et al. Optical imaging of pre-invasive breast cancer with a combination of VHHs targeting CAIX and HER2 increases contrast and facilitates tumour characterization. EJNMMI Res 2016;6:14. 10.1186/s13550-016-0166-y [PubMed: 26860296]
26. Oliveira S, Van Dongen GA, Stigter-van Walsum M, et al. Rapid visualization of human tumor xenografts through optical imaging with a near-infrared fluorescent anti-epidermal growth factor receptor nanobody. Mol Imaging 2012;11:33–46. [PubMed: 22418026]
27. Hoffman RM. Patient-derived orthotopic xenografts: better mimic of metastasis than subcutaneous xenografts. Nature Reviews Cancer 2015;15(8):451–452. 10.1038/nrc3972
28. De Vos J, Devoogdt N, Lahoutte T, Muyldermans S. Camelid single-domain antibody-fragment engineering for (pre)clinical in vivo molecular imaging applications: adjusting the bullet to its target. Expert Opin Biol Ther 2013;13:1149–1160. 10.1517/14712598.2013.800478 [PubMed: 23675652]
29. Muyldermans S, Baral TN, Retamozzo VC, et al. Camelid immunoglobulins and nanobody technology. Vet Immunol Immunopathol 2009;128:178–183. 10.1016/j.vetimm.2008.10.299 [PubMed: 19026455]
30. Ulrichts H, Silence K, Schoolmeester A, et al. Antithrombotic drug candidate ALX-0081 shows superior preclinical efficacy and safety compared with currently marketed antiplatelet drugs. Blood 2011; 118:757–765. 10.1182/blood-2010-11-317859 [PubMed: 21576702]
31. Hollifield AL, Arnall JR, Moore DC. Caplacizumab: an anti-von Willebrand factor antibody for the treatment of thrombotic thrombocytopenic purpura. Am J Health-Syst Pharm 2020;77:1201–1207. 10.1093/ajhp/zxaa151 [PubMed: 32588878]
32. le Besnerais M, Veyradier A, Benhamou Y, Coppo P. Caplacizumab: a change in the paradigm of thrombotic thrombocytopenic purpura treatment. Expert Opin Biol Ther 2019;19:1127–1134. 10.1080/14712598.2019.1650908 [PubMed: 31359806]
33. D'huyvetter M, De Vos J, Caveliers V, et al. Phase I trial of 131I-GMIB-Anti-HER2-VHH1, a new promising candidate for HER2-targeted radionuclide therapy in breast cancer patients. J Nucl Med Off Publ Soc Nucl Med 2020. 10.2967/jnumed.120.255679
34. Keyaerts M, Xavier C, Heemskerk J, et al. Phase I Study of 68Ga-HER2-nanobody for PET/CT assessment of HER2 expression in breast carcinoma. J Nucl Med Off Publ Soc Nucl Med 2016;57:27–33. 10.2967/jnumed.115.162024

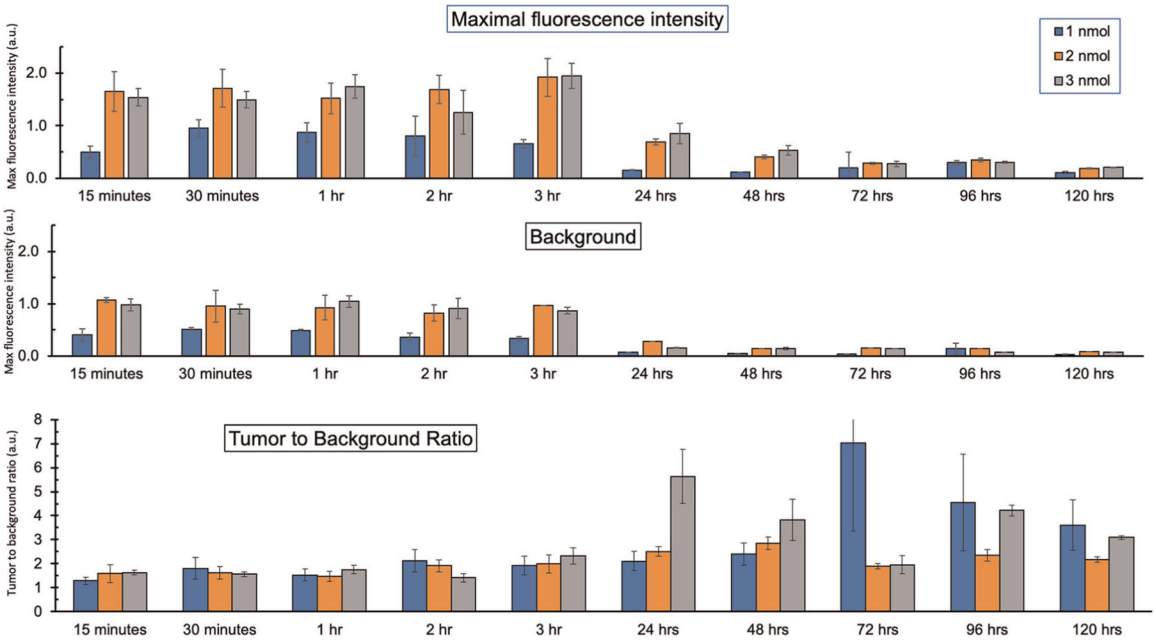

FIGURE 1.

Time course and dose-response evaluation of aCEA-nb-800 using LS174T colon cancer cell line-derived subcutaneous tumors. The mice were administered 1, 2, or 3 nmol of the tracer and maximal fluorescence intensity and surrounding tissue background were recorded with a LICOR Pearl small animal imager. Tumor to background ratios were calculated at the corresponding time intervals

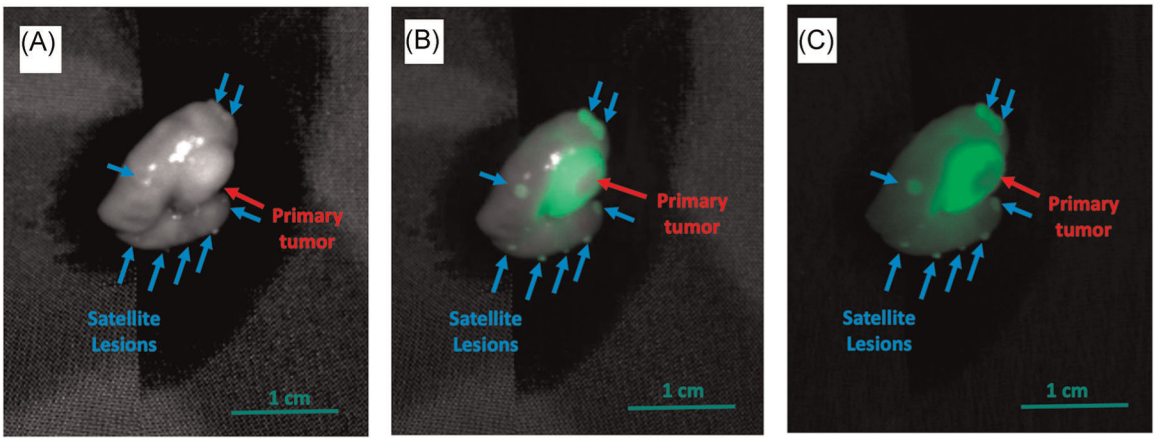

FIGURE 2.

The aCEA-nb-800 clearly labeled the primary colon tumor and satellite tumors in the LS174T colon cancer cell line-derived orthotopic tumor model. Three nanomoles of aCEA-nb-800 were injected intravenously and mice were sacrificed 3 h after injection and imaged with the LICOR Pearl small animal imager. Bright-light gray scale imaging shows the primary tumor with a red arrow (A) which is very difficult to visualize. Using fluorescence imaging, multiple sub-millimeter satellite tumors were detectable in the color-overlay mode (B) and the fluorescence signal only mode (C). Mean TBR for these lesions was 5.5 (*SEM* ± 1.30)

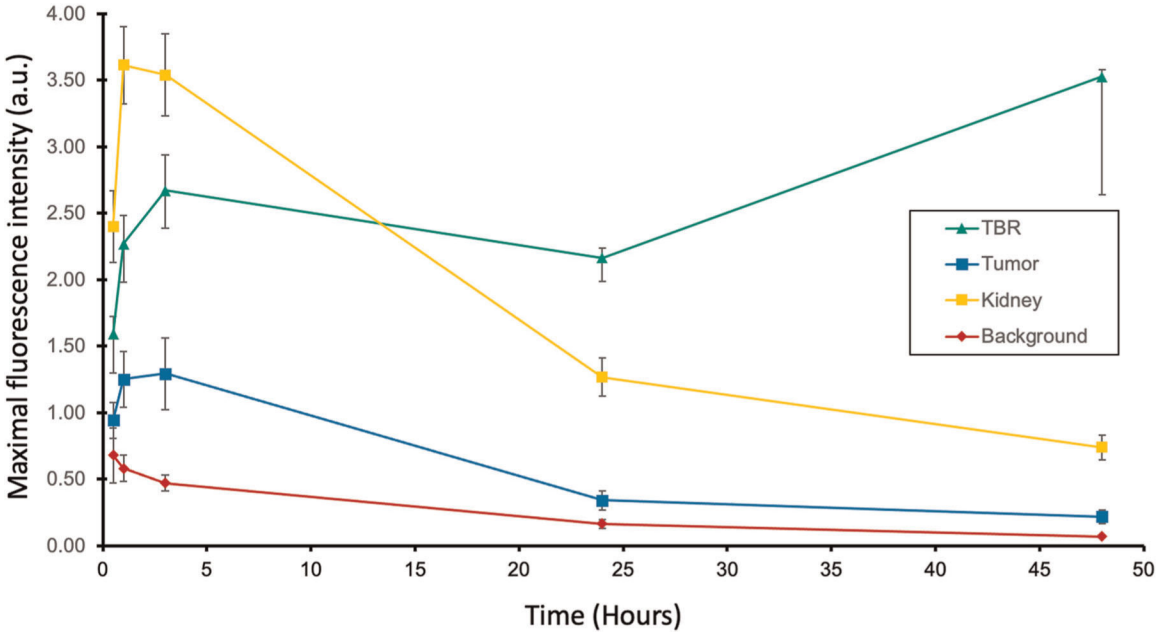

FIGURE 3.

Time course evaluation of aCEA-nb-800 using patient-derived colon cancer subcutaneous tumors. The mice were administered 3 nmol of the tracer and maximal fluorescence intensity at the tumor, kidney and the surrounding tissue background were recorded with a LICOR Pearl small animal imager. The tumor-to-background ratios were calculated at the corresponding time intervals

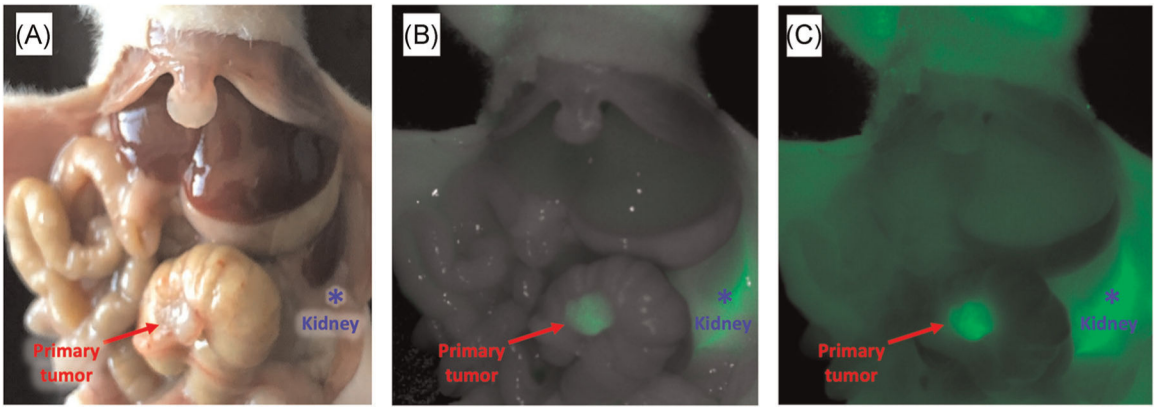

FIGURE 4.

The aCEA-nb-800 clearly labels the primary colon tumor and satellite lesions in a patient-derived orthotopic xenograft (PDOX) colon cancer model. Three nanomoles of aCEA-nb-800 were injected intravenously and mice were sacrificed 3 h after injection and imaged with a LICOR Pearl small animal imager. Bright-light imaging shows the primary tumor with a red arrow (A). Using fluorescence imaging, in the color-overlay mode (B) and the fluorescence signal only mode (C), the margin and tissue interface between normal colon and tumor are clearly visible. The kidney (blue asterisk) had a high fluorescence signal due to the renal elimination of aCEA-nb-800. Mean TBR for these lesions was 4.6 (*SEM* ± 1.47)